General remarks

The submitted manuscript investigates the electric current distribution within two magnetic dips identified as mirror mode structures in the terrestrial plasma sheet. As these are quasi-stationary magnetic field structures in the plasma frame, they must be supported by electric currents. According to the Authors, the currents are carried preponderantly by either electrons or ions, depending on the scale of the structure. To my knowledge this is the first experimental study of these current systems, therefore the manuscript can add a valuable contribution to our current understanding of the mirror modes. There are however a number of issues which should be addressed before publication.

Despite the availability of magnetic field and particle data from the four MMS spacecraft forming a "tetrahedron with inter-spacecraft distances of tens km" – as mentioned in page 2, line 79 of the manuscript, little advantage of the multi-point measurements is taken by the Authors. As far as I can tell, the multi-point capabilities of the MMS fleet were only used to determine the spacecraft-frame velocities of the detected compressional fluctuations (page 5-6, lines 113-120). Everywhere else, only single spacecraft data seems to be used. I am aware that the tetrahedron configuration might not be appropriate for some multi-point techniques, such as the curlometer, or that the characteristic size of the tetrahedron might not be ideal for the scale of the investigated structures. Nevertheless, the Authors should either use the measurements from all spacecraft or clearly explain why some of the data is excluded from the analysis. There is only a brief remark in this direction in the manuscript, stating that the interspacecraft distances are to small to allow an estimation of the magnetic field curvature (page 12, lines 270-272).

Even when essentially single spacecraft data are used (e.g. determining the principal coordinate system, scales of the structures, instability condition, current densities, pressures, particle velocities), reference should be made to all four MMS spacecraft, differences between spacecraft discussed, and when possible mean values used. In particular, figures 2 and 3 should include all spacecraft.

The text should be better structured and the language should be revised throughout the manuscript.

2 Specific comments

Page 2, line 37-39

Due to gradients in the magnetic field and plasma density, the mirror mode waves may slowly propagate relative to the ambient plasma flow (Hasegawa 1969, Pokhotelov JGRA 2003).

Answer: Thanks for your nice suggestion. We have added this sentence in our revised manuscript.

Page 5-6, line 115-120

More details about the timing method used to estimate the velocity of the compressional oscillations should be given. What are the time delays, accuracy? Tetrahedron size, elongation and planarity should be discussed. Is the determined speed the phase velocity in the spacecraft frame? (i.e. planar wave fronts orthogonal to the determined velocity vector are assumed? if yes, then the direction of the determined velocity vector should be compared with the minimum variance direction determined on page 7, line 153. They should agree.). Since the Authors refer to the oscillations between 20:51 and 21:04 (page 5, line 112) why only the interval [20:51:55, 20:53], corresponding to the later identified (page 7, Table 1) MM1 structure, is used? To ease the interpretation and comparison between the determined phase velocity vector and the mean plasma flow velocity, spherical coordinates (magnitude, θ, ϕ) should be used, and the angle between the two vectors should be given.

Answer: Thanks for your nice comments and suggestions. Burst magnetic field data (a resolution of 128 Hz) are available only between 20:51 and 20:54 UT, thus, we calculate the propagating velocity of the hole-like structure between 20:51:55 and

20:52:56 UT based on timing analysis (Harvey, 1998) to verify whether these compressional structures are non-propagation. Figure 2A shows the positions of the MMS spacecraft relative to MMS1 at 20:52 UT. The inter-spacecraft distances are ~13 to 21 km. Before performing the timing, the magnetic field data have been low-pass filtered with a cutoff period of 30 s to reduce the effect of high frequency fluctuations. Figure 2B shows the cross correlations between MMS1 and the three other satellites by using B_Z. The maximum correlation coefficients are all almost 1 between MMS1 and MMS2/3/4 with a lag time of -0.312 s, -0.164 s and -0.039 s, respectively. The estimated velocity is (71.3, 11.7°, -28°) in spherical coordinates (r, θ, φ) transferred from GSM coordinate system, where θ and φ are the longitude and latitude, respectively. By contrast, the average ion velocity is (71.6, 37.8°, -28.4°) in this interval. Comparing these two velocities, one can find that the compressional structures in Figure 1 are approximately stationary, i.e. they are mirror mode structures. The determined velocity is the phase velocity in the spacecraft frame, i.e. the front of the structure is supposed to be perpendicular to the determined velocity.

The minimum variance direction is supposed to be parallel to the above estimated velocity by timing, however, the angle between these two directions is ~37°. The MVA technique can be effected by waves or noises superimposed on the discontinuity surface, while the inter-spacecraft distances and configuration of the MMS satellites can effect on the accuracy of calculation, which might a possible explanation for the large difference between the two estimated normal directions.

We have added the above details in our revised manuscript.

(Harvey 1998) does not appear in the manuscript references list. I assume it is Chapter 12 in the ISSI “Analysis Methods for Multi Spacecraft Data” book.

Answer: Thanks for your nice comment. Yes, it is this reference. We have added the reference in our revised manuscript.

Page 6, line 127-135

The velocity used for estimating the scales (line 129) should be the one determined from timing analysis, not the plasma flow velocity. Since the two are not very different (line 118), this should not change much the results. Most probably the mirror mode structures have different sizes in different directions. For this study, the relevant size is the size in the direction orthogonal to the magnetic field. This size should be determined considering the angle between the mean magnetic field and the velocity vector determined from the timing analysis. Since the minimum variance direction – which should be close to the velocity direction – seems to be orthogonal to the mean magnetic field (figures 2 and 3), I expect that the sizes estimated in the manuscript are not far from the sizes in the orthogonal to the mean field direction. However, if the structures are not crossed through their centers – e.g. a path similar to the one shown in Figure 5 –, then the estimated sizes are only lower limits.

Answer: Thanks for your nice comment. Of course, it is better to use the velocity determined by timing to estimate the length scale of the mirror mode structure. The inter-spacecraft distances are ~13 to 21 km, which is too small to use the survey magnetic field data to do timing analysis. Only the burst magnetic field data during the first mirror mode structure are available, thus, we just do timing analysis for the first mirror mode structure to verify whether these structures are stationary in the ambient flow. Due to lack of sufficient burst magnetic field data, we estimate the length scale of the mirror mode structure in its cross-section using the M and N components of the ion velocity in our revised manuscript. It is difficult to verify whether the spacecraft trajectory crosses the center of the structure. Therefore, the estimated length is just the lower limits. We have added these details in our revised manuscript.

On lines 131-132 I assume the Authors meant “average ion perpendicular temperature”.

Answer: Thanks for your comment. Yes, we meant “average ion perpendicular temperature”. We have made a correction in our revised manuscript.

Page 7, Table 1

"ρ_i" should read "Scale (ρ_i)".

Answer: Thanks for your nice suggestion. In our paper, we mainly focus on the first and last mirror mode structures. And the information of these two structures have been written in the text. So, the table 1 is found to be not necessary to show, and has been deleted in our revised manuscript.

Page 7, lines 147-159

After line 147 the manuscript concentrates only on two magnetic dips (MM1 and MM5). To help readability, this should be clearly stated. The first structure (MM1) is analyzed in this paragraph and in the next one (up to line 181), while MM5 is analyzed in the remaining of the section. Dividing the text in subsections would improve readability. In this context, the maximum variance direction – which for magnetic mirrors should be aligned with the mean magnetic field – is the important direction. Therefore, the ratio between the maximum and the intermediate eigenvalues is relevant. The angles between the mean magnetic field and the determined **L**; **M** and **N** directions should be given.

The current density should be computed also using the curlometer, or the Authors should explain why this technique cannot be applied. Same comments apply for the MM5 on the next page.

Answer: Thanks for your nice comments and suggestions. We have separately analyzed these two mirror mode structures based on your suggestions. The angles between the mean magnetic field and the L, M and N directions are also given in the text. To study the relation between ions/electrons and the current density, the current density calculated by the curlometer method is a better choice. We determined the current density by the curlometer method, and did correlation analysis between the ion/electron velocity and the current density in our revised manuscript.

Figures 2 and 3 should show the orthogonal pressures of both ions and electrons. Are the ion velocities and the electron pressure in Figure 2 smoothed?

Answer: Thanks for your suggestions. We have shown the orthogonal pressures of both ions and electrons in these two figures. Only the electron data in these two figures have been smoothed within a 30-second window, since only electron data have significant high-frequency noise.

Page 7-8, lines 161-174

A more quantitative approach to determine which species (ions or electrons) contribute mostly to the electrical current is desirable. The Authors might e.g. compute the correlation between the electrical current and the ion and electron velocities.

Answer: Thanks for your nice suggestions. We have calculated the correlation coefficient between the electrical current and the ion/electron velocity in our revised manuscript. "The correlation coefficient between j_N and V_{eN} inside MM1 is -0.97." "The correlation coefficient between V_{iN} and j_N is 0.92 in the whole interval of MM2"

Page 11, lines 240-242

Please state the assumptions made for estimating the current density j_B.

Answer: Thanks for your nice suggestion. B_L changes ~5 nT in MM1 between 20:52:30 and 20:52:56 UT, and half of the estimated length of MM1 is 2.05×10^3 km in the cross-section. Assuming that B_M and B_N are 0, and B_L changes just along the trajectory of MMS, a current density j_B with a value of ~2 nA/m^2 in the cross-section is necessary to be self-consistent with the magnetic field depression. We stated the assumption in our revised manuscript.

Page 11, lines 251-255

There is no reference to chaotic particles in (Constantinescu 2002). Perhaps the Authors refer to another paper?

Answer: Thanks for your comment. We have corrected the reference, which is Büchner and Zelenyi (1989).

Büchner, J., and Zelenyi, L. M. Regular and chaotic charged particle motion in magnetotail like field reversals. Journal of Geophysical Research, 94, 11,821–11,842. https://doi.org/10.1029/JA094iA09p11821, 1989.

Page 12-13, lines 285-295

An estimation of the gradient drift velocities for electrons and ions (similar with the estimation done in the previous paragraph for MM1), as well as an estimation of the electron diamagnetic drift should be given.

Answer: Thanks for your comments. We use the data in the time interval between 21:02:30 and 21:02:50 UT to estimate the ion thermal pressure and magnetic gradients. Also, the average ion perpendicular and parallel temperatures, average total magnetic field and average curvature radius in this interval are used to estimate the velocities of the ion drift motions. Consequently, the velocities of the ion diamagnetic, magnetic gradient and curvature drift motions are ~17 km/s, 33 km/s and 79 km/s, respectively. By contrast, the velocities of the electron diamagnetic, magnetic gradient and curvature drifts are ~5 km/s, 14 km/s and 36 km/s. Since the ion diamagnetic and magnetic curvature drifts move almost in the same direction in the M-N plane, while the ion magnetic gradient drift moves in the opposite direction. Thus, the collective drift velocity is ~63 km/s, very close to the ion velocity inside MM2 with a speed of 70 km/s. Thus, one can expect that the bipolar V_{iN} in Figure 4 is the collective behaviors of the ion drift motions in MM2.

Page 13, lines 301-309

The normal directions (line 305) are almost orthogonal to each other. Knowing the estimated size between the entry and exit points, *d*, one can derive the transversal size of the structure as illustrated in Figure 5 (about 1*:*4*d*). Why is the MMS trajectory a curved line? Does the assumed relative motion of the magnetic structure change so much during the crossing time?

Answer: Thanks for your comments. "The normal directions are almost orthogonal to each other, the maximum length of MM2 in the cross-section could be 1.4 times the estimated length (6.6 ρ_i) based on the assumption of a circle." We found that the M component of the ion velocities V_{iM} at two edges of MM2 are different, so the MMS trajectory was drawn as a curved line. Actually, the difference V_{iM} at two edges of MM2 is not significant, so a straight line could be better to show the MMS trajectory. The trajectory has been changed to be a straight line in this figure in our revised manuscript.

General remarks

Wang et al. investigated the roles of electrons and ions in the formation of the current in the mirror mode structures in the plasma sheet using by the MMS observations. They found that the electrons and ions play a different role in the different sizes of mirror mode structures: the current carriers are mainly the electrons in small size mirror mode by magnetic gradient-curvature drift, and the ions in large size mirror mode by the ion diamagnetic drift. This study sheds new light on formation of currents in the mirror modes, and is worthy of publication in AG after moderate reversion.

In the discussion section: MMS consists of four identical spacecraft, and could provide the simultaneous measurements of four points. Why the authors use the plasma measurements and magnetic field to estimate the time series of magnetic gradient curvature drift, electron diamagnetic drift, ion diamagnetic drift, and other terms. I think this is useful to estimate these different terms and then compare them.

Line 18 It would be better to replace “data” to “instruments”, or remove “data”.

Answer: Thanks for your nice suggestions. We have removed “data” from this sentence.

Line 47-49 Actually the sizes of magnetic holes can be less than ion cyclotron radius in the magnetosheath. Such magnetic holes, named as kinetic-size magnetic hole or electron vortex magnetic hole, are widely observed using by MMS (doi:10.3847/1538-4357/ab0f2f, doi:10.1002/2017JA024415, doi.org/10.3847/1538-4357/aac831, doi:10.1002/2016JA023858).

Answer: Thanks for your comments. “Magnetic holes with a scale less than 1 ρ_i also exist in the magnetosheath as well as in the plasma sheet, and electron vortices are found inside these kinetic-size structures (Huang et al., 2017, 2018, 2019; Yao et al., 2017).” We have added these sentences in our revised manuscript.

Line 54-56 The small-size magnetic holes, below one ion cyclotron radius, are also detected in the plasma sheet (doi.org/10.3847/1538-4357/ab0f2f). These magnetic holes are always accompanied with electron scale instabilities, such as whistler waves.

Answer: Thanks for your comments. "Magnetic holes with a scale less than 1 ρ_i also exist in the magnetosheath as well as in the plasma sheet, and electron vortices are found inside these kinetic-size structures (Huang et al., 2017, 2018, 2019; Yao et al., 2017)." "Mirror mode structures accompanied by electron dynamics and whistler waves are also reported to occur during the dipolarization processes (Li et al., 2014; Huang et al., 2018)." We have added these sentences in our introduction.

Line 61-63 Dipolarization fronts are widely investigate in many literatures (doi:Âa10.1002/2015JA021083, doi:10.1029/2012GL051784, doi:10.5194/angeo-30-97-2012), and they play an important role in the energy conversion, mass transport, particle accelerations, and wave activities.

Answer: Thanks for your comments. "Dipolarization fronts (DFs), characterized by a sharp enhancement in B_Z in GSM, are formed ahead of the earthward fast flows (Ge et al., 2012; Wu et al., 2013; Schmid et al., 2016; Xiao et al., 2017). They play an important role in the energy conversion, mass transport, particle accelerations and wave activities (Fu et al., 2012; Huang et al., 2012, 2015)." We have added these sentences in our introduction.

Line 72-75: I suggest the author give the motivation of this paper to help the readers to better understand their work.

Answer: Thanks for your nice suggestion. "Our aim is to figure out whether the main contributor to the current inside the ion-scale mirror mode structure is the electron or ion." We have added this sentence to the last paragraph of the introduction.

Line 80-83 (Russell et al., 2014) should be corrected to (Russell et al., 2016). If the author did not use the burst mode data in this paper, I suggest the authors remove the introduction about the resolution of burst mode in this part.

Answer: Thanks for your suggestions and comments. We have made correction to the reference. We have also deleted the description about the burst mode data in the introduction.

Line 115-117 Why are the data performed low-pass filtered before the timing analysis? I suggest the authors give some descriptions here.

Answer: Thanks for your nice suggestions. Waves with a period of several to ~20 s can be found inside the magnetic dip in Figure 3. To reduce the effect of high frequency fluctuations, the data have been performed low-pass filtered before the timing analysis. We have given descriptions in our revised manuscript.

Line 120 “tends to be larger” “increases” or “has a peak”?

Answer: Thanks for your comments. We meant that the ion number density has a peak in the trough of the oscillations. To better descript the relation between the number density and the total magnetic field, we have changed this sentence to “The total magnetic field varies in anti-phase with the ion number density during this interval.”

Line 131: how to calculate the local ion gyro radius? Which time interval? Please give the details in the text.

Answer: Thanks for your comments and suggestions. The local ion gyro radius is calculated by the average ion perpendicular temperature and the average magnetic field magnitude between 20:51:55 – 20:52:56 UT. We have given more details in our revised manuscript.

133-135 Why the range of the scale and the angle are inconsistent with those in table 1? The "rotation angle" is the "shear angle"?

Answer: Thanks for your comments. The angle is the angle between the magnetic field directions at two edges of each structure. The inconsistency here is caused by a typo. We have revised it in our manuscript. Since we mainly focus on the first and last mirror mode structures, and the information in table 1 can be found in the text, so table 1 is not necessary now and we have deleted it in our revised manuscript.

Line 155: As the authors know, the separation of the four MMS spacecraft is very small. Thus, one can use the curlometer method to estimate the current density based on the magnetic field from four spacecraft. Why not the author use this method to calculate the current and compare with the current derived from the plasma measurements?

Answer: Thanks for your comments and suggestions. The current density can be determined by the plasma moments or the curlometer method. To study the relation between ions/electrons and the current density, the current density calculated by the curlometer method is a better choice. So, we calculated the current by the curlometer in our revised manuscript. And we compared the current with the electron/ion velocity, and found a strong relationship between the current and the electron or ion velocity.

Line 192 J_N should be corrected to J_M.

Answer: Thanks for your comments. We have revised it in our manuscript.

Line 216: "Ion velocities" should be "Ion velocities Vi_md"?

Answer: Thanks for your comments. We have revised it in our manuscript.

Line 230-235 The pileup region usually exists behind the DFs, not ahead of the DFs, for example the definition of flux pileup region in the paper (doi:10.1029/2012JA018141). In addition, the mirror mode structures are observed after the detection of DF. Why the authors thought they originate from the pileup region ahead of the DF?

Answer: Thanks for your suggestions. Yes, the flux pileup region usually occurs behind the DF, and the region ahead of the DF is called the pressure pileup region. I have changed "the pileup region" to "the pressure pileup region".

Since mirror mode structures are stationary in the ambient flow, we can estimate the distance of the structures relative to the DF in the Y direction using the average V_Y ~30 km/s during the structures. Thus, they are likely to occur dawnside of the MMS spacecraft with a distance of ~4 R_E in the Y direction when the spacecraft are crossing the DF at around 20:38 UT. Compared this distance with the typical size of the DF (~3 R_E) (Huang et al., 2015) and the size of the structures, the mirror mode structures might come from the dawnside flank of the DF. Since the DF is considered to be a tangential discontinuity (Schmid et al., 2019) which pushes the background plasma to its flanks (Fu et al., 2012a, 2012b; Liu et al., 2013; Birn et al., 2015), the plasma near the flank is expected to come from the pressure pileup region ahead of DFs. In addition, mirror mode structures have been reported to be potentially generated in such a pressure pileup region (Zieger et al., 2011; Wang et al., 2016). Thus, the mirror mode structures in Figure 1 might originate from the pressure pileup region ahead of the DF.

Line 243 Please indicate at which time "The amplitude of the bipolar j_N in MM1 is ~2 nA/m^2".

Answer: Thanks for your suggestions. We have added the time interval in this sentence.

Line 247 It would be better to add "in MM5" after "electron velocity"

Answer: Thanks for your suggestion. We have revised it based on your suggestion.

Line 271-272 The authors can try to use the magnetic field from four MMS spacecraft to estimate the curvature radius of mirror modes.

Answer: Thanks for your suggestion. Using the data from all four MMS satellites, we can determine the curvature of MM1 by

$$\rho_c = B^{-2}B_i\nabla_i B_j - B^{-4}B_j B_i B_l \nabla_i B_l$$

where the indices i, j and l indicates the three components of the magnetic field, and B = |B| (Shen et al., 2003). The curvature radius R_C is $1/\rho_c$. We have estimated the curvature radius of the mirror mode structures, and discussed it in our revised manuscript.

Line 286-187 Did the authors ever calculate the magnetic gradient drift velocity in MM5? It would be necessary to compare the magnetic gradient drift velocity and the Vi_N.

Answer: Thanks for your suggestion. We use the data in the time interval between 21:02:30 and 21:02:50 UT to estimate the ion thermal pressure and magnetic gradients. Also, the average ion perpendicular and parallel temperatures, average total magnetic field and average curvature radius in this interval are used to estimate the velocities of the ion drift motions. Consequently, the velocities of the ion diamagnetic, magnetic gradient and curvature drift motions are ~17 km/s, 33 km/s and 79 km/s, respectively. Since the ion diamagnetic and magnetic curvature drifts move almost in the same direction in the M-N plane, while the ion magnetic gradient drift moves in the opposite direction. Thus, the collective drift velocity is ~63 km/s, very close to the ion velocity inside MM2 (which is MM5 in our previous manuscript) with a speed of 70 km/s.

Line 304-307 Did the authors compare the normal directions calculated by MVA and timing method to ensure the accuracy of the results.

Answer: Thanks for your suggestion. Comparing the normal directions determined by MVA and timing method can ensure the accuracy of the results. However, no burst magnetic field data are available in this time interval. So, we did not compare the normal directions calculated by both methods in our manuscript.

Line 307-309 Please indicate which MMS? 1 or 2 or 3 or 4 after “trajectory of MMS”. How to deduce the possible trajectory of MMS, please give details in the text.

Answer: Thanks for your comments and suggestions. Since the inter-spacecraft distances of MMS are very small compared to the scale of this mirror mode structure, the trajectory of the four MMS satellites are almost the same. Therefore, we only draw the trajectory of MMS1 in this figure. Based on the studies about the geometry of the mirror mode structure, we assume that the cross-section of the mirror mode structure is a circle. According to the normal directions of the both half sides of the structure and the ambient flow direction, we can simply get the possible trajectory of MMS1. We have added these details in our revised manuscript.

Line 316 Please add a color bar in Figure 5.

Answer: Thanks for your suggestion. We have added a color bar in this Figure.

Roles of electrons and ions in formation of the current in mirror mode structures in the terrestrial plasma sheet: MMS observations

Guoqiang Wang[1, 2], Tielong Zhang[1, 3], Mingyu Wu[1], Daniel Schmid[3], Yufei Hao[4], Martin Volwerk[3]

[1]Institute of Space Science and Applied Technology, Harbin Institute of Technology, Shenzhen, China
[2]Key Laboratory of Lunar and Deep Space Exploration, Chinese Academy of Sciences, Beijing, China
[3]Space Research Institute, Austrian Academy of Sciences, Graz, Austria
[4]Key Laboratory of Planetary Sciences, Purple Mountain Observatory, Chinese Academy of Sciences, Nanjing, China

Abstract

Mirror mode structures widely exist in various space plasma environments. ~~Currents are believed to exist in mirror mode structures and to be self-consistent with the magnetic field depression.~~ Here, we investigate a train of mirror mode structures in the terrestrial plasma sheet on 11 August 2017 ~~measured by~~based on the Magnetospheric Multiscale mission~~ data~~. We find that~~ a~~ bipolar current densities exist~~s~~ in the cross-section of two hole-like mirror mode structures, referred to as magnetic dips. The bipolar current density in the magnetic dip with a size of ~~~3~~ 2.2 ρ_i (the ion gyro radius) is mainly contributed by variations of the ~~an~~ electron ~~bipolar~~ velocity, which is mainly formed by the magnetic gradient-curvature drift. For another magnetic dip with a size of ~6.~~67~~ 6 ρ_i, the bipolar current density is mainly caused by an ion bipolar velocity, which can be explained by the collective behaviors of the ion ~~diamagnetic~~ drift motions. The current density inside the mirror dip contributes to the maintenance of the hole-like structure's stable. ~~These~~ Our observations suggest that the electrons and ions play different roles in the formation of currents in magnetic dips with different sizes.

1 Introduction

Mirror modes are pressure-balanced and compressional magnetic structures (Hasegawa, 1969; Tsurutani et al., 2011; Wang et al., 2016; Zhang et al., 2018). They widely exist in many space plasma regions, such as solar wind (Zhang et al., 2008, 2009; Russell et al., 2009), planetary magnetosheath (Volwerk et al., 2008; Schmid et al., 2014), planetary magnetosphere (Vaivads et al., 2001; Rae et al., 2007), and comets (Glassmeier et al., 1993; Volwerk et al., 2016). These structures are believed to be generated by the mirror instability excited in the mirror unstable environment (Hasegawa, 1969; Southwood and Kivelson, 1993). The plasma perpendicular temperature anisotropy provides free energy to excite the mirror instability (Kivelson and Southwood, 1996). Once the mirror mode structures are generated, they will convected with the ambient flow since they are non-propagating relative to the ambient flow (Tsurutani et al., 2011). Due to gradients in the magnetic field and plasma density, the mirror mode structure may slowly propagate relative to the ambient plasma flow (Hasegawa, 1969, Pokhotelov et al., 2003). It is expected that they will stop to grow or decay when they move into the mirror stable region. Actually, they are reported to be able to survive in the mirror stable region in the solar wind and magnetosheath (Balikhin et al., 2009; Russell et al., 2009).

Mirror mode structures appears as not only quasi-periodic sinusoidal oscillations, but also local enhancements or decrease of the magnetic field intensity, referred to as magnetic peaks or dips (Tsurutani et al., 2011). Magnetic peaks can only exist in the mirror unstable environments, while magnetic dips are able to survive in the mirror stable region (Kuznetsov et al., 2007; Soucek et al., 2008). The typical scales of the mirror mode structures are 10s ρ_i in the magnetosheath (Tsurutani et al., 1982; Horbury and Lucek, 2009), where ρ_i is the ion gyro radius. Based on observations of the four Cluster satellites, the longest scales of the mirror mode structures in the magnetosheath is found to be 2 – 6 times length of their shortest scales, and their shapes are approximately cigar-like (Horbury and Lucek, 2009). By contrast, magnetic dips with a scale less than 1 ρ_i also exist in the magnetosheath as well as in the plasma sheet, and electron vortices are found inside the structure (Huang et al., 2017, 2018, 2019; Yao et al., 2017).

In the terrestrial plasma sheet, there also exist mirror mode structures with several ion gyro radii (Vaivads et al., 2001; Zieger et al., 2011; Li et al., 2014; Wang et al., 2016). The earthward fast flows can result in a magnetic pileup in its leading area, and the ion perpendicular temperature anisotropy in the pileup region is able to make the local plasma conditions mirror-unstable to generate mirror mode structures (Zieger et al., 2011). Mirror mode structures accompanied by electron dynamics and whistler waves are also reported to occur during the dipolarization processes~~ in the plasma sheet~~ (Li et al., 2014; Huang et al., 2018). Dipolarization fronts (DFs), characterized by a sharp enhancement in B_Z in GSM, are formed ahead of the earthward fast flows (Ge et al., 2012; Wu et al., 2013; Schmid et al., 2016; Xiao et al., 2017). They play an important role in the energy conversion, mass transport, particle accelerations and wave activities (Fu et al., 2012b; Huang et al., 2012, 2015b). They are able to create a pressure ~~magnetic~~ pileup region ahead of the DF when moving earthward (Schmid et al., 2011; ~~Fu et al., 2012;~~ Liu et al., 2013). Mirror mode structures with a scale of ~4 ρ_i are reported to occur in the pressure ~~magnetic~~ pileup region ahead of a DF, and the mirror instability is suggested to be a potential mechanism to generate these structures since local environments are mirror-unstable (Wang et al., 2016). Within a mirror mode structure there should be an electric current driven by the magnetic gradient and curvature drifts of the ions and/or electrons in order to sustain their stability (Constantinescu, 2002).

In this study, we investigate a train of ion-scale mirror mode structures in the terrestrial plasma sheet on 11 August 2017 using the Magnetospheric Multiscale (MMS) mission data. ~~The~~ Our aim ~~of this study~~ is to figure out whether the main contributor to the current density inside the ion-scale mirror mode structure is the ~~roles of~~ electron or

~~s and~~ ions~~ in the current inside the mirror mode structure based on the high-resolution MMS data~~.

2 Observation

The MMS spacecraft consist of four identical satellites, which constitute a tetrahedron with inter-spacecraft distances of tens km (Burch et al., 2015). In the present study, we use the survey (a resolution of 16 Hz) ~~and burst (128 Hz)~~ magnetic field data obtained by the Fluxgate Magnetometer (Russell et al., ~~2014~~2016), and the survey (4.5 s) ~~and burst (150 ms for ions, 30 ms for electrons)~~ plasma data recorded by the Fast Plasma Instrument (Pollock et al., 2016).~~ Since the burst magnetic and plasma data are only available in parts of the interval in Figure 1, the survey data are used throughout the paper unless stated otherwise.~~

2.1 Overview of a DF event

Figure 1 shows that B_Z sharply increases ~8 nT within 7 seconds ~~at ~20:38 UT on 11 August 2017~~ accompanied by a fast earthward flow with a maximum ~~velocity~~ speed of ~~~300~~ 397 km/s at ~20:38 UT on 11 August 2017. Also, the local ion beta, the ratio of the ion thermal pressure to the magnetic pressure is ~4, and the elevation angle ($\theta = \arctan\left(\frac{B_Z}{\sqrt{B_X^2+B_Y^2}}\right)$) changes ~50° with a maximum angle of 64° (not shown). These observations satisfy the criteria of the DF from Fu et al. (2012a), indicating that it is a DF event shown as the vertical dotted line at around 20:38 UT in Figure 1. At 20:40 UT, the MMS spacecraft are located near (-18, 14.6, 2) R_E in GSM (Geocentric Solar Magnetospheric coordinates, used everywhere unless otherwise stated). The normal direction of the DF is (0.34, 0.82, -0.46) determined by the minimum variance analysis (MVA) (Sonnerup and Scheible, 1998) using the data in the interval between 20:37:33 and 20:37:42 UT. The ratio of the intermediate to minimum eigenvalues (λ_2/λ_3) is ~15, indicating that the estimated normal direction is reliable (Volwerk, 2006; Wang et al., 2014). The estimated normal direction suggests that the MMS spacecraft are located at the duskward side of the DF based on the semi-circle assumption of the DF (Huang et al., 2015a).

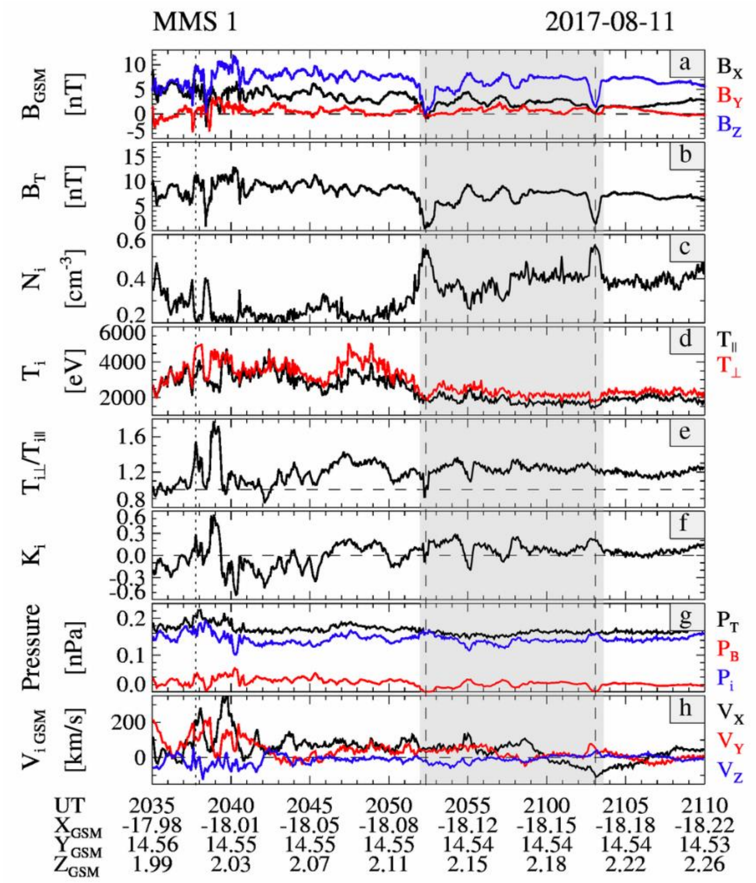

Figure 1. Observations of a DF event by MMS 1 on 11 August 2017. From top to bottom: three components of the magnetic field in GSM (a), the total magnetic field (b), ion density (c), ion perpendicular (red) and parallel (black) temperatures (d), ion perpendicular temperature anisotropy (e), the threshold of the mirror instability (f), the magnetic, ion thermal and total pressures (g), and three components of the ion velocity in GSM (h). The gray shadow indicates several compressional structures. The vertical dotted line indicates the DF, and the dashed lines indicate~~s~~ the trough of ~~each~~ two ~~compressional structure~~hole-like structures. ~~The gray shadows indicate the mirror mode structures.~~

Several quasi-periodic compressional magnetic oscillations with a period of ~2 min are observed in the interval between 20:51 and 21:04 UT shown as the gray region in Figure 1. The total magnetic field varies in anti-phase with the ion number density during this interval. In addition, the total pressure, sum of the magnetic and ion thermal pressures, is almost constant, indicating that they are pressure-balanced structures. The threshold of the ion mirror instability K_i is shown in Figure 1f, where $K = \frac{T_{\perp}}{T_{\parallel}} - 1 - \frac{1}{\beta_{\perp}}$, and $T_{\perp}$, $T_{/\!/}$, and $\beta_{\perp}$ are perpendicular and parallel ion temperatures and perpendicular ion beta, respectively (Southwood, and Kivelson, 1993). Local plasma environments become mirror unstable and can excite ion mirror instabilities when $K_i > 0$. The maximum K_i in each ~~mirror mode~~ compressional structure reaches over 0.2, and it tends to decrease to near or below 0 from the center of each structure to its edge. Before 20:51 UT or after 21:04 UT, K_i is near or below 0, i.e. the background environment for these structures is ~~mirror~~ marginally mirror stable.

The above properties of the compressional structures indicate that they are likely to be mirror mode structures (Tsurutani et al., 2011). Mirror mode structures are supposed to be non-propagating structures relative to the ambient flow if there are no significant gradients in the magnetic field and plasma density (Pokhotelov et al., 2003). Burst magnetic field data (a resolution of 128 Hz) are available only between 20:51 and 20:54 UT, thus, we perform timing analysis (Harvey, 1998) to calculate the propagating velocity of the hole-like structure between 20:51:55 and 20:52:56 UT to verify whether these compressional structures are non-propagation. Figure 2A shows the positions of the MMS spacecraft relative to MMS1 at 20:52 UT. The inter-spacecraft distances are ~13 to 21 km. Before performing the timing, the magnetic field data have been low-pass filtered with a cutoff period of 30 s to reduce the effect of high frequency fluctuations. Figure 2B shows the cross correlations between MMS1 and the three other satellites by using B_Z. The maximum correlation coefficients are all almost 1 between MMS1 and MMS2/3/4 with a lag time of -0.312 s, -0.164 s and -0.039 s, respectively. The estimated velocity is (71.3, 11.7°, -28°) in spherical coordinates (r, θ, φ) transferred from GSM coordinate system, where θ and φ are the longitude and latitude, respectively. By contrast, the average ion velocity is (71.6, 37.8°, -28.4°) in this interval. Comparing these two velocities, one can find that the compressional structures in Figure 1 are approximately stationary, i.e. they are mirror mode structures.

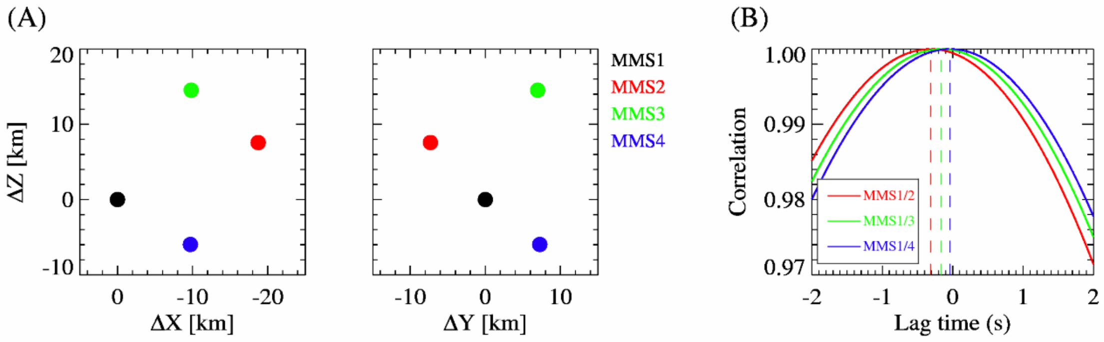

Figure 2. (A) Positions of the MMS spacecraft relative to MMS1 at 20:52 UT in the X-Z (left) and Y-Z (right) planes. (B) The cross correlations between MMS1 and the three other MMS satellites calculated by using B_Z in the interval 20:52:55 – 20:52:56 UT.

~~Since waves with a period of ~20 s are superimposed on the compressional oscillations, and only burst magnetic field data are available before 20:53 UT for this interval, we estimate the velocities of these compressional oscillations by timing analysis (Harvey, 1998) using the burst magnetic field data low-pass filtered with a cutoff period of 30 s between 20:51:55 and 20:53 UT. The estimated velocity is (61.6, 12.7, -33.5) km/s, which is close to the average ion velocity (49.3, 38.2, -35.2) km/s in this interval, suggesting that these oscillations are approximately stationary in the ambient flow. The ion number density tends to be larger in the trough of the oscillations as the dashed lines shown in Figure 1. Figure 1g shows that the magnetic and ion thermal pressures vary in anti-phase during the compressional oscillations, in addition, the total pressure is almost constant, indicating that the oscillations are pressure-balanced. The above properties of the compressional oscillations indicate that they are mirror mode structures (Tsurutani et al., 2011).~~

The first and last mirror mode structures as the dashed lines shown in Figure 1 are hole-like, which are referred to as magnetic dips. We will focus on these two magnetic dips in the rest paper, and we mark them as MM1 (20:51:55 – 20:52:56 UT) and MM2 (21:02:26 – 21:03:34 UT).

2.2 Plasma properties in MM1

To further look at the plasma properties in the magnetic dips, we transform the ion and electron velocities as well as the magnetic field and current density into the principal axis (LMN) coordinate system as shown in Figure 3. The principal axes vectors are calculated by MVA using the magnetic field data obtained from MMS1 in the interval between 20:51:55 and 20:52:56 UT. To reduce the effect of the high frequency fluctuations, the magnetic field data have been low-pass filtered with a cutoff period of 30 s before performing the MVA analysis. The **L**, **M** and **N** directions are (0.46, 0.27, 0.85), (0.28, 0.86, -0.42) and (-0.84, 0.43, 0.32) in GSM, respectively. The eigenvalue ratio λ_2/λ_3 is ~9.

We mark these mirror mode structures as MM1 to MM5, and their time intervals and scales are listed in Table 1. The scales are estimated by

$$\sqrt{\left(\int_{t_1}^{t_2} V_X dt\right)^2 + \left(\int_{t_1}^{t_2} V_Y dt\right)^2 + \left(\int_{t_1}^{t_2} V_Z dt\right)^2}$$

where V_X, V_Y and V_Z are three components of the ion velocity, while t_1 and t_2 are the start and end time of each structure (Ge et al., 2011). And the local ion gyro radius ρ_i is estimated by the average ion temperature and average total magnetic field low-pass filtered with a cutoff period of 20 s. The scales of these structures vary between ~3 ρ_i and 14.38 ρ_i. The rotation angle of the magnetic field over each structure varies between ~2.5 ° and 12.4 °.

The threshold of the ion mirror instability K_i is shown in Figure 1f, where $K = \frac{T_\perp}{T_\parallel} - 1 - \frac{1}{\beta_\perp}$, and $T_\perp$, $T_\parallel$, and $\beta_\perp$ are perpendicular and parallel ion temperatures and perpendicular ion beta, respectively (Southwood, and Kivelson, 1993). Local plasma environments become mirror unstable and can excite ion mirror instabilities when $K_i >$ 0. The maximum K_i in each mirror mode structure reaches over 0.2, and it tends to decrease to near or below 0 from the center of each structure to its edge. Before 20:51 UT or after 21:04 UT, K_i is near or below 0, i.e. the background environment for these

~~structures is mirror marginal stable.~~

~~**Table 1.** The time interval, angle of the magnetic field at two edges, scale, and maxima threshold of the ion mirror instability for each mirror mode structure.~~

	~~Time interval (HH:MM:SS)~~	~~θ (°)~~	~~ρ_i~~	~~Scale (km)~~	~~K_i_max~~
~~MM1~~	~~20:51:55 – 20:53:06 UT~~	~~13.3~~	~~3~~	~~4.83×10^3~~	~~0.2~~
~~MM2~~	~~20:53:06 – 20:55:00 UT~~	~~6.3~~	~~14.41~~	~~11.32×10^3~~	~~0.28~~
~~MM3~~	~~20:55:00 – 20:57:14 UT~~	~~4.6~~	~~12.36~~	~~8.25×10^3~~	~~0.17~~
~~MM4~~	~~20:57:14 – 20:58:56 UT~~	~~6.3~~	~~12.93~~	~~8.39×10^3~~	~~0.25~~
~~MM5~~	~~21:02:26 – 21:03:34 UT~~	~~2.9~~	~~6.67~~	~~6.42×10^3~~	~~0.23~~

~~MM1 and MM5 appear as hole-like structure, which are referred to as magnetic dips (Tsurutani et al., 2011). To further look at the plasma properties in the magnetic dips, we transform the ion and electron velocities as well as the magnetic field and current density into the principal axis (LMN) coordinate system. The principal axes vectors are calculated by the minimum variance analysis (MVA, Sonnerup and Scheible, 1998) in the interval between 20:51:55 and 20:53:06 UT. The **L**, **M** and **N** directions are (0.44, 0.17, 0.88), (0.33, 0.88, -0.34) and (-0.84, 0.44, 0.33) in GSM, respectively. The ratio of the intermediate to minimum eigenvalues is ~4.7, indicating that the MVA results are reliable (Sergeev et al., 2003). The current density is calculated by $\mathbf{j} = qn_e(\mathbf{V}_i - \mathbf{V}_e)$, where n_e, V_i, and V_e are electron number density, ion velocity and electron velocity, respectively. To reduce the effect of the high-frequency oscillations, the magnetic field, electron velocity and current density in Figure 2 (also in Figure 3) have been smoothed within a 20-second window.~~

Figure ~~2~~ 3 shows that B_L is dominant while B_M and B_N vary around 0~~,~~. The angles between the average magnetic field in this interval and the **L**, **M** and **N** directions are ~18°, 108° and 87°, respectively. It ~~indicating~~ indicates that the cross-section of ~~the structure~~MM1 is approximately parallel to the M-N plane, and is approximately perpendicular to the ambient magnetic field. The N direction is supposed to be parallel to the above estimated velocity by timing, however, the angle between these two directions is ~37°. The MVA technique can be effected by waves or noises superimposed on the discontinuity surface (Lepping and Behannon, 1980; Schmid et al., 2019), while the inter-spacecraft distances and configuration of the MMS spacecraft can effect on the accuracy of calculation (Harvey, 1998), which might a possible explanation for the large difference between the two estimated normal directions. The ion velocity is mainly in the M-N plane during the whole interval, and there are no significant changes in both V_{iM} and V_{iN}. By contrast, the N component of the electron velocity V_{eN} shows a bipolar variation with an amplitude maximum change of ~70 40 km/s. To reduce the effect of the high frequency noise, the electron data have been smoothed within a 30-second window in Figure 3 as well as in Figure 4. Interestingly, Aan enhancement (a decrease) of V_{eN} occurs in the left (right) side of MM1, i.e. a bipolar feature appears in V_{eN}. One can also note that the maximum and minimum of V_{e_N} in MM1 tend to occur near the maximum gradient of B_L. V_{e_M} also shows a bipolar variation in MM1 compared to the ambient value. In addition

The current density in Figure 3 is calculated by the curlometer technique (Dunlop et al., 2002) using the magnetic field data low-pass filtered with a cutoff period of 30 s. The current density can be regarded as reliable when the ratio $|\nabla \cdot B|/|\nabla \times B|$ is less than 0.2. T, the N and M components of the current density j_N shows a bipolar variations similar to V_{eN} the electron velocity with an opposite trend of change. The correlation coefficient between j_N and V_{eN} inside MM1 is -0.97. By comparing the variations in the ion and electron velocities, one can note that the bipolar current density inside MM1 is mainly determined associated with by the the electron velocity. One can also note that tThe maximumpeak and minimumtrough of the bipolar V_{eN} in MM1 tend to occur near the maximum gradient of B_L., The bottom panel in Figure 2 shows the electron perpendicular thermal pressure $P_{e\perp}$, and there while there is no significant change in $P_{e\perp}$ in MM1.

Since the magnetic dips are stationary in the ambient flow, we can estimate their scale in the cross-section by

$$\sqrt{\left(\int_{t_1}^{t_2} V_M dt\right)^2 + \left(\int_{t_1}^{t_2} V_N dt\right)^2}$$

where V_M and V_N are the M and N components of the ion velocity, t_1 and t_2 are the start and end times of each magnetic dip. The scale of MM1 is estimated to be ~4.1 × 10^3 km, or ~2.2 ρ_i, where ρ_i is the local ion gyro radius calculated by the average ion perpendicular temperature and the average B_T in MM1 between 20:51:55 – 20:52:56 UT. Since the spacecraft may not cross the center of the magnetic dip, the estimated scale is the lower limit.

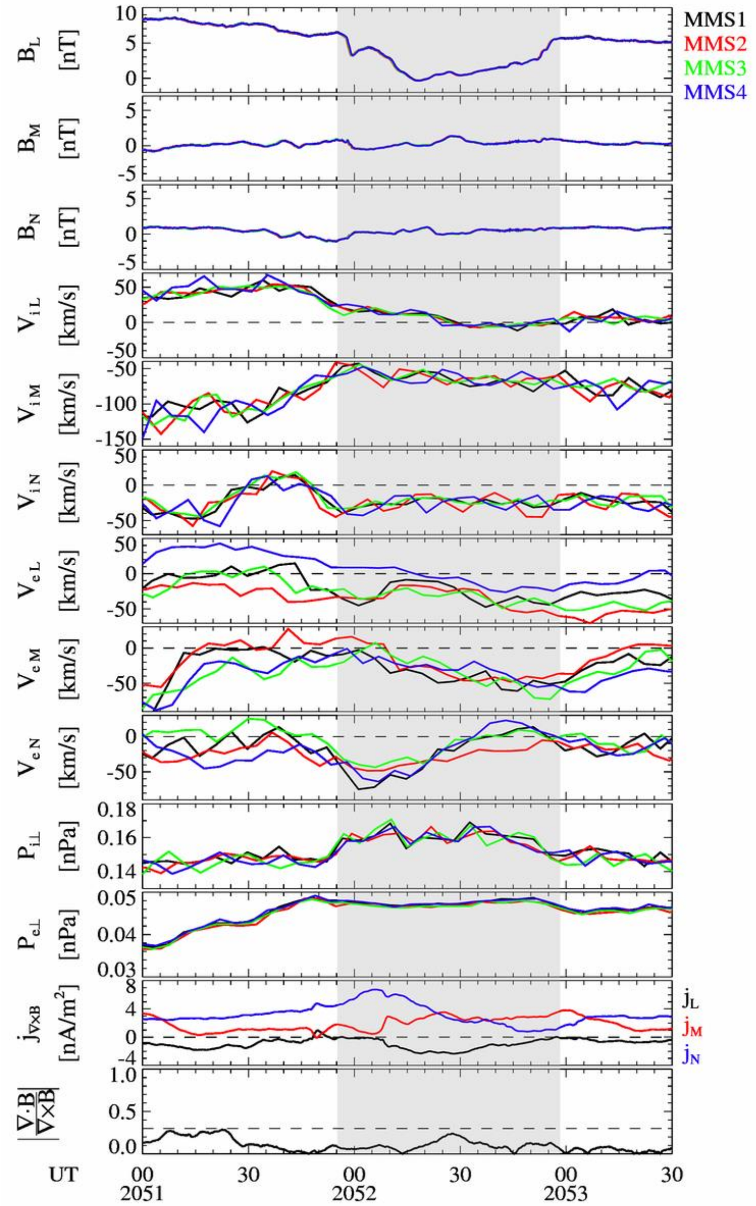

Figure ~~2~~**3.** From top to bottom: Three components of the magnetic field, ion and electron velocities in LMN, the ion and electron perpendicular thermal pressures, the current density in LMN and the ratio of |∇•B|/|∇ × B|~~the principal axis (LMN) coordinate system, and electron perpendicular thermal pressure~~ between 20:51 and 20:53:30 UT. The black, red, green and blue colors indicate data obtained from MMS1, MMS2, MMS3 and MMS4, respectively. The current density is calculated by the curlometer technique. The gray region indicates the interval of the magnetic dip.

2.2 Plasma properties in MM2

Figure ~~3~~ 4 shows the magnetic field, ion velocity, electron velocity and current density in LMN between 21:01 and 21:05 UT ~~and ion perpendicular thermal pressure in MM5~~. The magnetic field data between 21:02:~~30~~ 26 and 21:03:~~30~~ 34 UT are used to calculate the principal axes vectors by MVA ~~(Sonnerup and Scheible, 1998)~~. The ratio λ_2/λ_3 ~~of the intermediate to minimum eigenvalues~~ is ~6.~~8~~, and the **L**, **M** and **N** directions are (0.26, 0.~~09~~1, 0.96), (-0.~~49~~44, 0.~~87~~89, 0.~~05~~02) and (-0.~~83~~86, -0.~~49~~43, 0.~~27~~28) ~~in GSM~~, respectively. The angles between the average magnetic field in this interval and the **L**, **M** and **N** directions are ~1.5°, 89° and 89°, respectively. B_L is dominant during the whole interval, while B_M and B_N are very small. Thus, the cross-section of ~~MM5~~ MM2 is also approximately parallel to the M-N plane, and almost perpendicular to the ambient magnetic field. No large-amplitude fluctuations appear in MM2 compared to MM1. The ion velocity V_{iM} and V_{iN} are dominant, while V_{iL} varies around 0. Interestingly, a bipolar feature in V_{iN} with a variation up to ~~73~~ 80 km/s (peak minus trough) can be distinctly found inside the dip, while V_{iM} tends to increase compared to the ambient flow. V_{iN} is smaller (larger) than the ambient value in the left (right) side of the dip. The peak and trough of the bipolar V_{iN} appear when there are significant gradients in the magnetic field and the ion perpendicular thermal pressures. It indicates that the bipolar V_{iN} could be associated with the magnetic gradient and diamagnetic drifts. The length of MM2 in the cross-section is estimated to be ~6.4 × 10^3 km, or ~6.6 ρ_i.

The current density in Figure 4 is also determined by the curlometer technique. Before performing the curlometer analysis, the magnetic field data have been low-pass filtered with a cutoff period of 20 seconds to reduce the effect of the high-frequency fluctuations. One can find that j_N shows a similar bipolar feature to V_{iN}. The correlation coefficient between V_{iN} and j_N is 0.92 in the whole interval of MM2, indicating that both parameters have a strong relation. The peak minus the trough of j_N during MM2 is ~5.6 nA/m^2. J_N also shows a similar bipolar feature with a variation up to 5.4 nA/m^2, By contrast, while J_L-j_L and J_N-j_M have no such a clear bipolar featureno significant changes. The electron velocities show variations with periods larger than 1 minute, but no clear bipolar feature appears in any component of the electron velocity during MM2The N component of the electron velocity, however, shows no such characteristics, indicating that the bipolar J_N-j_N is mainly determined by the bipolar V_{iN}. The ion perpendicular thermal pressure $P_{i\perp}$ in the structure is obviously larger than the ambient value, and $P_{i\perp}$ tends to be larger from the edge to the center of MM5.

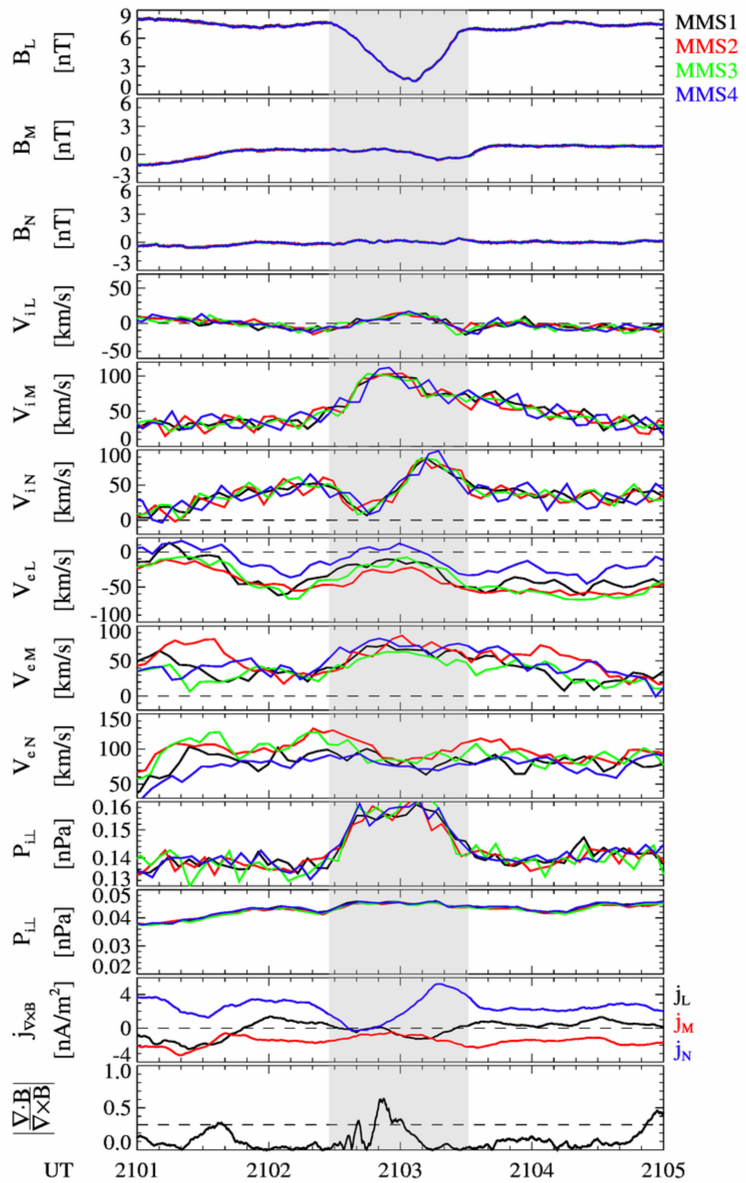

Figure ~~3~~4. ~~Three components of the magnetic field, ion and electron velocities, current density in the principal axis (LMN) coordinate system, and ion perpendicular thermal pressure between 2101 and 2105 UT.~~From top to bottom: Three components of the magnetic field, ion and electron velocities in LMN, the ion and electron perpendicular thermal pressures, the current density in LMN and the ratio of |∇•B|/|∇ × B| between 21:01 and 21:05 UT. The black, red, green and blue colors indicate data obtained from MMS1, MMS2, MMS3 and MMS4, respectively. The current density is calculated by the curlometer technique. The gray region indicates the interval of the magnetic dip.

To look at the variations of the ion flow in ~~MM5~~MM2, we assume that the ion velocity observed during ~~MM5~~ MM2 consists of $\mathbf{V}_{i\_a}$ and $\mathbf{V}_{i\_md}$, where $\mathbf{V}_{i\_a}$ is the ambient ion velocity, and $\mathbf{V}_{i\_md}$ is the ion velocity inside ~~the magnetic dip~~MM2 relative to the ambient flow. The average velocity 30 seconds before and after ~~MM5~~ MM2 is selected to be regarded as $\mathbf{V_{i\_a}}$ with a value of (-2.6, 51.4, 33.4) km/s in LMN. Figure ~~4~~ 5 shows the deflection of $\mathbf{V_{i\_md}}$ in the M-N plane. The arrows indicate the direction of the ion velocity, and their lengths indicate the magnitude of $\mathbf{V_{i\_md}}$ in the M-N plane. The direction of $\mathbf{V_{i\_md}}$ gradually changes from around -60° to 50° in the M-N plane. Also, the strength of $\mathbf{V_{i\_md}}$ in this plane gradually increases and then decreases from the left side of the magnetic dip to the right side. In addition, the N component of $\mathbf{V_{i\_md}}$ changes from negative to positive at just around the center of the structure.

Figure ~~4~~5. Ion velocities $\mathbf{V_{i\_md}}$ in the M-N plane during ~~MM5~~MM2. The arrows indicates the direction of the ion velocities, and their lengths indicate the amplitude of the ion velocities. And the gray line indicates the total magnetic field of ~~MM5~~MM2.

3 Discussion

~~Figure 1 shows the ambient plasma is marginally mirror stable, indicating that the mirror mode structures are not locally generated.~~ Since mirror mode structures ~~they~~ are stationary in the ambient flow, we can estimate the distance of the structures relative to the DF in the Y direction using the average V_Y ~30 km/s during the structures. ~~t~~Thus, they are ~~estimated~~ likely to occur dawnside of the MMS spacecraft with a distance of ~4 R_E in the Y direction when the spacecraft are crossing the DF at around 20:38 UT~~,~~ ~~where the average V_Y ~30 km/s during the structures are used~~. Compared this distance with the typical size of the DF (~3 R_E) (Huang et al., 2015a) and the size of the ~~structures~~magnetic dips in Figure 1, the mirror mode structures might come from the dawnside flank of the DF. Since the DF is considered to be a tangential discontinuity

(Schmid et al., 2019) which pushes the background plasma to its flanks (Fu et al., 2012a, 2012b; Liu et al., 2013; Birn et al., 2015), the plasma near the flank is expected to come from the pressure pileup region ahead of DFs. In addition, m~~M~~irror mode structures have been reported to ~~occur~~ be potentially generated in such a pressure pileup region (Zieger et al., 2011; Wang et al., 2016). ~~The pileup of the magnetic field and the ion reflection ahead of the DF are suggested to provide free energy to excite the ion mirror instability (Zieger et al., 2011; Wang et al., 2016).~~ Thus, the mirror mode structures in Figure 1 might originate from the pressure pileup region ahead of the DF.

Based on Ampère's law, there should exist a current in the magnetic dip to sustain the structure's stability~~, and the current is determined by the collective behavior of electrons and ions~~ (see Constantinescu, 2002). Figure ~~2~~ 3 and ~~3~~ 4 shows that a bipolar current density is observed in both MM1 and ~~MM5~~MM2. B_L changes ~~~6~~ 5 nT in MM1 between 20:52:30 and 20:52:56 UT, and half of the estimated length of MM1 is ~~4~~2.~~83~~05 × 10^3 km in the cross-section. Assuming that B_M and B_N are 0, and B_L changes just along the trajectory of MMS, ~~Thus,~~ a current density j_B with a value of ~2 nA/m^2 in the cross-section is necessary to be self-consistent with the magnetic field depression. The amplitude of the bipolar j_N ~~in MM1~~ is ~2 nA/m^2 between 20:52:30 and 20:52:56 UT, almost equal to j_B, indicating that MM1 is a stable structure (Constantinescu, 2002). Similarly, ~~MM5~~ MM2 is also a stable structure. ~~The variations of the current density in MM1 is mainly contributed by the variations of the electron velocity. By contrast, no significant changes occur in the electron velocity, while a bipolar ion velocity similar to the current density appears in V_{iN}. Thus, the bipolar current density in MM5 is mainly contributed by the variations of the ion velocity.~~

Significant changes can be found in electron velocities in MM1, while the three components of the ion velocity are almost constant. Therefore, the current density in MM1 is mainly contributed by electrons. The amplitude of the bipolar electron velocity in V_{eN} is ~40 km/s (see Figure 3). Three kind of the electron drift motions are expected to create the current density, i.e. the magnetic gradient drift, the magnetic curvature drift and the diamagnetic drift. The electron perpendicular thermal pressure $P_{e\perp}$ changes ~0.002 nPa in MM1, the average electron number density is ~0.4 cm^{-3}, and the average total magnetic field is ~3 nT. Consequently, the estimated electron diamagnetic drift velocity is ~4 km/s, much smaller than the amplitude of the bipolar V_{eN}. The peak of the bipolar V_{eN} occurs in the time interval between 20:52:40 and 20:52:50 UT, during which there are no significant magnetic field fluctuations. We select this time interval to estimate the velocities of the magnetic gradient and curvature drifts. The total magnetic field changes ~1.1 nT, and the median total magnetic field is ~2.2 nT in this interval. The median electron perpendicular and parallel temperatures are ~680 eV and 650 eV. The length scale of MM1 is ~4.1 $\times 10^3$ km in the M-N plane and its duration is ~61 s, thus the length for the time interval between 20:52:40 and 20:52:50 UT is ~680 km. Using the data from all four MMS satellites, we can determine the curvature of MM1 by

$$\rho_c = B^{-2} B_i \nabla_i B_j - B^{-4} B_j B_i B_l \nabla_i B_l$$

where the indices i, j and l indicates the three components of the magnetic field, and B = |**B**| (Shen et al., 2003). The curvature radius R_C is $1/\rho_C$. Before performing the calculation, the magnetic field data have been low-pass filtered with a cutoff period of 1 second to reduce the effect of the high-frequency noise. The median R_C in this interval is 1.1 $\times 10^3$ km. Thus, the velocities of the electron magnetic gradient and curvature drifts are ~209 km/s and 262 km/s, respectively. Since the magnetic curvature drift in MM1 is in the opposite direction of the magnetic gradient drift., thus the collective velocity of these two velocities are ~53 km/s, which is close to the amplitude of the bipolar V_{eN}. It suggests that the bipolar electron velocity in MM1 is mainly formed by the electron magnetic gradient and curvature drifts.

Figuring out the magnetic field geometry, we can get the exact values of the magnetic gradient and curvature drifts. Due to the small interspacecraft distance among the MMS satellites, it is difficult to get a reasonable magnetic field geometry and a reliable curvature radius of MM1. Nevertheless, it is expected that both the magnetic gradient and curvature drifts contribute significantly to the formation of the current in MM1.

The size of MM1 is ~2.2 ρ_i, and its central magnetic field strength is almost 0. Thus, the ion gyro radius is expected to significantly change within one orbit, and ions would randomly jump between neighboring magnetic dips. These ions are referred to as chaotic particles (Büchner and Zelenyi, 1989), which could be one reason why ions do not seem to contribute to the formation of the current in MM1.

The size of MM1 is ~3 ρ_i, and its central magnetic field strength is almost 0. Thus, the ion gyro radius is expected to significantly change within one orbit, and ions would randomly jump between neighboring magnetic dips (Constantinescu, 2002). These ions are referred to as chaotic particles, which do not contributed to the formation of the current in the mirror mode structure (Constantinescu, 2002). It might be an important reason that the current in MM1 is mainly contributed by electrons. The size of MM1 is ~20 ρ_e, where ρ_e is the local electron gyro radius. Thus, a quasi-hydrodynamic treatment can be used to describe the electrons. Three kind of drifts are expected to form the current in MM1, i.e. the magnetic gradient drift, the magnetic curvature drift, and the electron diamagnetic drift. The electron perpendicular thermal pressure $P_{e\perp}$ changes ~0.002 nPa in MM1, the average electron number density is ~0.4 cm^{-3}, and the average total magnetic field is ~3 nT. Consequently, the estimated electron diamagnetic drift velocity is ~4 km/s, much smaller than the bipolar amplitude ~70 km/s in V_{e_N} in Figure 2. We also calculate the magnetic gradient drift velocity with an estimated value of 1.13 $\times 10^2$ km/s, where the electron perpendicular temperature is ~800 eV, and B_L changes ~6 nT in a length of 2.45 $\times 10^2$ km. Figure 2 shows that the strength of the bipolar velocity in V_{e_N} is ~70 km/s, smaller than the magnetic gradient drift velocity. The magnetic curvature drift in MM1 is in the opposite direction of the magnetic gradient drift. Figuring out the magnetic field geometry, we can get the exact values of the magnetic gradient and curvature drifts. Due to the small interspacecraft distance among the MMS satellites, it is difficult to get a reasonable magnetic field geometry and a reliable curvature radius of MM1. Nevertheless, it is expected that both the magnetic gradient and curvature drifts contribute significantly to the formation of the current in

~~MM1.~~

No significant changes occur in the electron velocity in MM2, thus the bipolar current density is mainly contributed by the variations of the ion velocity (see Figure 4). The size of ~~MM5~~ MM2 is ~6.6~~7~~ ρ_i, larger than that of MM1. ~~The ion bipolar velocity in MM5 indicates a local ion flow, suggesting there exists some magnetohydrodynamic properties in this structure.~~ The trough of the bipolar V_{iN} is observed at around 21:02:45 UT, meanwhile, V_{iM} increases ~50 km/s compared to the ambient flow on the left side of MM2. The amplitude of the bipolar V_{iN} is ~50 km/s, thus, the ion velocity inside MM2 ~70 km/s relative to the ambient ion flow. The ion perpendicular thermal pressure tends to be larger from the edge of ~~MM5~~ MM2 towards its center (see Figure ~~3~~4), therefore, an ion diamagnetic drift is expected to be formed (Baumjohann and Treumann, 1996). We use the data in the time interval between 21:02:30 and 21:02:50 UT to estimate the ion thermal pressure and magnetic gradients. Also, the average ion perpendicular and parallel temperatures, average total magnetic field and average curvature radius in this interval are used to estimate the velocities of the ion drift motions. Consequently, the velocities of the ion diamagnetic, magnetic gradient and curvature drift motions are ~17 km/s, 33 km/s and 79 km/s, respectively. By contrast, the velocities of the electron diamagnetic, magnetic gradient and curvature drifts are ~5 km/s, 14 km/s and 36 km/s. Since the ion diamagnetic and magnetic curvature drifts move almost in the same direction in the M-N plane, while the ion magnetic gradient drift moves in the opposite direction. Thus, the collective drift velocity is ~63 km/s, very close to the ion velocity inside MM2 with a speed of 70 km/s. Thus, one can expect that the bipolar V_{iN} in Figure 4 is the collective behaviors of the ion drift motions in MM2.

~~The ion perpendicular thermal pressure changes by ~ 0.013 nPa for intervals 21:02:31 – 21:02:40 UT and 21:03:07 – 21:03:29 UT (see Figure 4). Using the average ion density and magnetic field strength, the estimated velocities of the diamagnetic drift are 40.4 km/s and 19.2 km/s for these two intervals, which is comparable with the~~

~~amplitude of the bipolar V_{iN} in Figure 3. Therefore, the ion bipolar velocity as well as the bipolar current in MM5 is mainly contributed by the ion diamagnetic drift. It is expected that the magnetic gradient and curvature drifts of ions move in opposite directions in MM5. We speculate that the difference of the magnetic gradient and curvature drift velocities are small possibly resulting from the magnetic field geometry of MM5. The larger scale of MM5 compared to MM1 could reduce the magnetic gradient and electron thermal pressure gradient resulting in slower magnetic gradient drift and electron diamagnetic drift velocities. That's could be the reason why no significant bipolar occurs in the electron velocity in MM5. Another possible reason might the magnetic field geometry which might reduce the difference of the magnetic gradient and curvature drift velocities of electrons.~~

Except for the bipolar V_{iN}, ~~One can note that~~ there is an enhancement of V_{iM} in ~~MM5~~MM2. To figure out the variations of V_{iM} and V_{iN} in ~~MM5~~MM2, we analyze the possible trajectory of the MMS spacecraft crossing ~~MM5~~MM2. Mirror mode structures in the magnetosheath are found to be cigar-like structures instead of sheets or tubes (Constantinescu et al., 2003; Horbury and Lucek, 2009). To simplify our analysis, we assume that the cross-section of ~~the MM5~~ MM2 ~~structure~~ is a circle. To be self-consistent with the magnetic field depression, the ion flow as well as the current is supposed to be clockwise as the black arrows shown in Figure ~~5~~6. Based on the normal directions of the both half sides of the structure along the spacecraft trajectory and the ambient flow direction, we can get the possible trajectory of the MMS spacecraft in the M-N plane. We calculate the normal directions of the two sides of MM2 ~~the magnetic dip~~ by MVA, and the values are (0.03, 0.79, 0.61) and (-0.05, -0.65 0.76) in LMN for the intervals 21:02:30 – 21:03 and 21:03:10 – 21:03:25 UT, respectively. The ratios of the intermediate to minimum eigenvalues λ_2/λ_3 are 6.4 and 8.5, respectively. The normal directions are almost orthogonal to each other, thus, the maximum length of MM2 in the cross-section could be 1.4 times the estimated length (6.6 ρ_i) based on the assumption of a circle. The velocity of the ambient ion flow is (-2.6, 51.4, 33.4) km/s in LMN. Thus, ~~we can get~~ a possible trajectory of MMS in the M-N plane can be drawn based on the ambient flow and the above normal directions as the red arrow shown in Figure ~~5~~6. Since the inter-spacecraft distances are very small compared to the scale of MM2, only the possible trajectory of MM1 is shown in Figure 6. Along the trajectory, ~~one can note that~~ V_{iN}~~the N component of the ion velocity~~ changes from negative to positive from one to another side of ~~MM5~~MM2, while V_{iM} ~~the M component~~ is positive, which is in agreement with the deflection of the ion flow shown in Figure ~~4~~5. Thus, the variations of V_{iM} and V_{iN} are consistent with the prediction of the ion vortex in the cross-section. ~~indicates a ring-like flow in the cross-section of MM5.~~ Such a ring-like flow might play an important role in the evolution of the mirror mode structure or maintaining the stability of the magnetic dip.

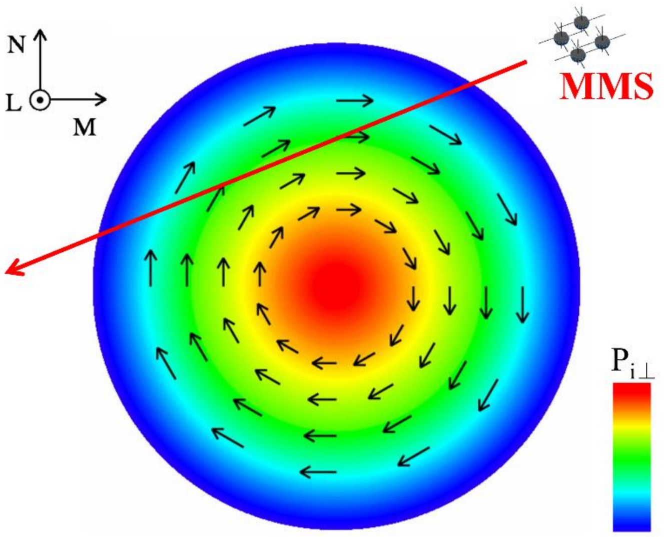

Figure ~~5~~6. Schematic of MMS1 crossing the magnetic dip in the M-N plane. The colors changing from center (red) of the magnetic dip to its edge (blue) indicate the decrease of the ion perpendicular thermal pressure as shown by the color bar. The back arrows in the magnetic dip indicate the direction of the ion velocity. The red arrow indicates a possible trajectory of MMS1.

4 Summary

We have studied the ion-scale mirror mode structures ~~with a size of several to 14.41 ρ_i~~ in the plasma sheet on 11 August 2017. ~~Current is expected to exist in the magnetic dip contributed by the collective behavior of electrons and ions. Our observations show~~

~~a bipolar current in two magnetic dips, and the electrons and ions play different roles in each dip.~~ We find that a ~~The~~ bipolar current density in the magnetic dip with a size of ~~~3~~ 2.2 ρ_i is mainly contributed by an electron bipolar velocity in the cross-section. The electron bipolar ~~electron~~ velocity ~~could mainly~~mainly results from the magnetic gradient and curvature drifts~~ of electrons~~. The chaotic motion of ions might be one significant reason that ions have almost no contribution to the formation of the bipolar current in this magnetic dip. For another magnetic dip with a size of 6.6~~7~~ ρ_i, the bipolar current is mainly contributed by the ion bipolar velocity, which can be explained by the collective behavior of the ion ~~diamagnetic~~ drift ~~velocity~~motions. And the variations of the ion velocity in the cross-section suggest the potential existence of the ion vortex. We suggest that ~~both~~ the scale ~~and~~ as well as the magnetic geometry of the magnetic dip~~s~~ ~~are~~ is significant to determine the roles of electrons and ions in the formation of the current inside the dip~~s~~.

References

Balikhin, M. A., Sagdeev, R. Z., Walker, S. N., Pokhotelov, O. A., Sibeck, D. G., Beloff, N., and Dudnikova, G.: THEMIS observations of mirror structures: Magnetic holes and instability threshold, Geophys. Res. Lett., 36, https://doi.org/10.1029/2008GL036923, 2009.

Baumjohann, W., and Treumann, R. A.: Basic Space Plasma Physics, Imperial Coll. Press, London, pp. 147-149, 1997.

Birn, J., Runov, A., and Hesse, M.: Energetic ions in dipolarization events, J. Geophys. Res.-Space, 120, 7698–7717, doi:10.1002/2015JA021372, 2015.

Büchner, J., and Zelenyi, L. M.: Regular and chaotic charged particle motion in magnetotail like field reversals, J. Geophys. Res., 94, 11,821–11,842. https://doi.org/10.1029/JA094iA09p11821, 1989.

Burch, J. L., Moore, T. E., Torbert, R. B., and Giles, B. L.: Magnetospheric multiscale overview and science objectives, Space Sci. Rev., 199, 5–21, 2015.

Constantinescu, O. D.: Self-consistent model for mirror structures, J. Atmos. Sol. Terr. Phys, 64, 645–649, 2002.

Constantinescu, O. D., Glassmeier, K. H., Treumann, R., and Fornacon, K. H.: Magnetic mirror structures observed by Cluster in the magnetosheath, Geophys. Res. Lett., 30, 4–1, 2003.

Fu, H. S., Khotyaintsev, Y. V., Vaivads, A., André, M., and Huang, S. Y.: Occurrence rate of earthward-propagating dipolarization fronts, Geophys. Res. Lett., 39, https://doi.org/10.1029/2012GL051784, 2012a.

Fu, H. S., Khotyaintsev, Y. V., Vaivads, A., André, M., Sergeev, V. A., Huang, S. Y., Kronberg, E. A., and Daly, P. W.: Pitch angle distribution of suprathermal electrons behind dipolarization fronts: A statistical overview, J. Geophys. Res., 117, A12221, doi:10.1029/2012JA018141, 2012b.

Harvey, C. C.: Spatial gradients and the volumetric tensor, in Analysis Methods for Multi-Spacecraft Data, ISSI Sci. Rep. SR-001, edited by G. Paschmann and P. W. Daly, pp. 307–322, Int. Space Sci. Inst., Bern, 1998.

Hasegawa, A.: Drift mirror instability in the magnetosphere, Phys. Fluids, 12, 2642–2650, 1969.

Huang, S. Y., Zhou, M., Deng, X. H., Yuan, Z. G., Pang, Y., Wei, Q., Su, W., Li, H. M., Wang, Q. Q.: Kinetic structure and wave properties associated with sharp dipolarization front observed by Cluster, Ann. Geophys., 30, 97–107, doi:10.5194/angeo-30-97-2012, 2012.

Huang, S. Y., Fu, H. S., Vaivads, A., Yuan, Z. G., Pang, Y., Zhou, M., Khotyaintsev, Yuri V., Deng, X. H., André, M., Zhang, L., Fu, S., Li, H. M., and Wang, D. D.: Dawn-dusk scale of dipolarization front in the earth's magnetotail: multi-cases study, Astrophys. Space Sci., 357, 1–7, https://doi.org/10.1007/s10509-015-2298-3, 2015a.

Huang, S. Y., et al.: Electromagnetic energy conversion at dipolarization fronts: Multispacecraft results, J. Geophys. Res.-Space, 120, 4496–4502, doi:10.1002/2015JA021083, 2015b.

Huang, S. Y., et al.: A statistical study of kinetic-size magnetic holes in turbulent magnetosheath: MMS observations, J. Geophys. Res.-Space, 122, 8577–8588, doi:10.1002/2017JA024415, 2017.

Huang, S. Y., Sahraoui, F., Yuan, Z. G., Le Contel, O., Breuillard, H., He, J. S., Zhao, J. S., Fu, H. S., Zhou, M., Deng, X. H., Wang, X. Y., Du, J. W., Yu, X. D., Wang, D. D., Pollock, C. J., Torbert, R. B., Burch, J. L.: Observations of Whistler Waves Correlated with Electron-scale Coherent Structures in the Magnetosheath Turbulent Plasma, The Astrophysical Journal, 861:29 (5pp), https://doi.org/10.3847/1538-4357/aac831, 2018.

Huang, S. Y., He, L. H., Yuan, Z. G., Sahraoui, F., Le Contel, O., Deng, X. H., Zhou, M., Fu, H. S., Jiang, K., Yu, X. D., Li, H. M., Deng, D., Pollock, C. J., Torbert, R. B., Burch, J. L.: MMS Observations of Kinetic-size Magnetic Holes in the Terrestrial Magnetotail Plasma Sheet, The Astrophysical Journal, 875:113 (8pp), https://doi.org/10.3847/1538-4357/ab0f2f, 2019.

Horbury, T. S., and Lucek, E. A.: Size, shape, and orientation of magnetosheath mirror mode structures, J. Geophys. Res., 114, https://doi.org/10.1029/2009JA014068, 2009.

Ge, Y. S., McFadden, J. P., Raeder, J., Angelopoulos, V., Larson, D., and Constantinescu, O. D.: Case studies of mirror-mode structures observed by THEMIS in the near-Earth tail during substorms, J. Geophys. Res., 116, https://doi.org/10.1029/2010JA015546, 2011.

Ge, Y. S., Zhou, X. Z., Liang, J., Raeder, J., Gilson, M. L., Donovan, E., Angelopoulos, V., and Runov, A.: Dipolarization fronts and associated auroral activities: 1. Conjugate observations and perspectives from global MHD simulations, J. Geophys. Res., 117, https://doi.org/10.1029/2012JA017676, 2012.

Glassmeier, K., Motschmann, U., Mazelle, C., Neubauer, F., Sauer, K., Fuselier, S., and Acua, M.: Mirror modes and fast magnetoacoustic waves near the magnetic pileup boundary of comet P/Halley, J. Geophys. Res., 98, 20,955–20,964, https://doi.org/10.1029/93JA02582, 1993.

Kivelson, M. G., and Southwood, D. J.: Mirror instability: 2. The mechanism of nonlinear saturation, J. Geophys. Res., 101, 17,365–17,371, https://doi.org/10.1029/96JA01407, 1996.

Kuznetsov, E. A., Passot, T., and Sulem, P. L.: Dynamical Model for Nonlinear Mirror Modes near Threshold, Phys. Rev. Lett., 98(23), https://doi.org/10.1103/PhysRevLett.98.235003, 2007.

Lepping, R. P., and Behannon, K. W.: Magnetic field directional discontinuities: 1. Minimum variance errors. J. Geophys. Res., 85, 4695–4703. https://doi.org/10.1029/JA085iA09p04695, 1980.

Li, H., Zhou, M., Deng, X., Yuan, Z., and Huang, S.: Electron dynamics and wave activities associated with mirror mode structures in the near-Earth magnetotail, Sci. China-Technol. Sci., 57(8), 1541–1551, https://doi.org/10.1007/s11431-014-5574-5, 2014.

Liu, J., Angelopoulos, V., Zhou, X. Z., Runov, A., and Yao, Z. H.: On the role of pressure and flow perturbations around dipolarizing flux bundles, J. Geophys. Res.-Space, 118, 7104–7118, https://doi.org/10.1002/2013JA019256, 2013.

Pollock, C., Moore, T., Jacques, A., et al.: Fast plasma investigation for magnetospheric multiscale, Space Sci. Rev., 199, 331–406, 2016.

Pokhotelov, O. A., Sandberg, I., Sagdeev, R. Z., Treumann, R. A., Onishchenko, O. G., Balikhin, M. A., and Pavlenko, V. P.: Slow drift mirror modes in finite electron-temperature plasma: Hydrodynamic and kinetic drift mirror instabilities, J. Geophys. Res., 108(A3), 1098, doi:10.1029/2002JA009651, 2003.

Rae, I. J., Mann, I. R., Watt, C. E. J., Kistler, L. M., and Baumjohann, W.: Equator-S observations of drift mirror mode waves in the dawnside magnetosphere, J. Geophys. Res., 112, https://doi.org/10.1029/2006JA012064, 2007.

Russell, C. T., Blanco‐Cano, X., Jian, L. K., and Luhmann, J. G.: Mirror‐mode storms: STEREO observations of protracted generation of small amplitude waves, Geophys. Res. Lett., 36, 2009.

Russell, C., Anderson, B., Baumjohann, W., Bromund, K., Dearborn, D., Fischer, D., Le, G., Leinweber, H., Leneman, D., Magnes, W., et al.: The magnetospheric multiscale magnetometers, Space Sci. Rev., 199, 189–256, 2016.

Schmid, D., Volwerk, M., Nakamura, R., Baumjohann, W., and Heyn, M.: A statistical and event study of magnetotail depolarization fronts, Ann. Geophys., 29(9), 1537–1547, https://doi.org/10.5194/angeo-29-1537-2011, 2011.

Schmid, D., Volwerk, M., Plaschke, F., Vörös, Z., Zhang, T. L., Baumjohann, W., and Narita, Y.: Mirror mode structures near Venus and Comet P/Halley, Ann. Geophys., 32, 651–657, https://doi.org/10.5194/angeo-32-651-2014, 2014.

Schmid~~1~~, D., Nakamura, R., Volwerk, M., Plaschke, F., Narita, Y., Baumjohann, W., Magnes, W., Fischer, D., Eichelberger, H. U., Torbert, R. B., Russell, C. T., Strangeway, R. J., Leinweber, H. K., Le, G., Bromund, K. R., Anderson, B. J., Slavin, J. A., and Kepko, E. L.: A comparative study of dipolarization fronts at MMS and Cluster, Geophys. Res. Lett., 43, 6012-6019, https://doi.org/10.1002/2016GL069520, 2016.

Schmid D., Volwerk, M., Plaschke, F., Nakamura, R., Baumjohann, W., Wang, G. Q., Wu, M. Y., Zhang, T. L.: Dipolarization fronts: tangential discontinuities? On the spatial range of validity of the MHD jump conditions, J. Geophys. Res.-Space, 124. https://doi.org/10.1029/2019JA027189, 2019.

Sergeev, V., Runov, A., Baumjohann, W., Nakamura, R., Zhang, T. L., Volwerk, M., Balogh, A., Rème, H., Sauvaud, J. A., André, M., and Klecker, B.: Current sheet flapping motion and structure observed by Cluster, Geophys. Res. Lett., 30(6), 1327, doi:10.1029/2002GL016500, 2003.

Sonnerup, B. U. Ö., and Scheible, M.: Minimum and maximum variance analysis, ISSI Sci. Rep. Ser., 1, 185–220, 1998.

Soucek, J., Lucek, E., and Dandouras, I.: Properties of magnetosheath mirror modes observed by Cluster and their response to changes in plasma parameters, J. Geophys. Res., 113, https://doi.org/10.1029/2007JA012649, 2008.

Southwood, D. J., and Kivelson, M. G.: Mirror instability: 1. The physical mechanism of linear instability, J. Geophys. Res., 98, 9181–9187, 1993.

Tsurutani, B. T., Smith, E. J., Anderson, R. R., Ogilvie, K. W., Scudder, J. D., Baker, D. N., and Bame, S. J.: Lion roars and nonoscillatory drift mirror waves in the

magnetosheath, J. Geophys. Res., 87, 6060–6072, https://doi.org/10.1029/JA087iA08p06060, 1982.
Tsurutani, B. T., Lakhina, G. S., Verkhoglyadova, O. P., Echer, E., Guarnieri, F. L., Narita, Y., and Constantinescu, D. O.: Magnetosheath and heliosheath mirror mode structures, interplanetary magnetic decreases, and linear magnetic decreases: Differences and distinguishing features, J. Geophys. Res., 116, https://doi.org/10.1029/2010JA015913, 2011.
Vaivads, A., Baumjohann, W., Haerendel, G., Nakamura, R., Kucharek, H., Klecker, B., Lessard, M. R., Kistler, L. M., Mukai, T., and Nishida, A.: Compressional Pc5 type pulsations in the morningside plasma sheet, Ann. Geophys., 19, 311–320, https://doi.org/10.5194/angeo-19-311-2001, 2001.
Volwerk, M.: Multi-satellite observations of ULF waves, in Magnetospheric ULF Waves: Synthesis and New Directions, edited by K. Takahashi et al., pp. 109–135, AGU, Washington, D. C, 2006.
Volwerk, M., Zhang, T. L., Delva, M., Vörös, Z., Baumjohann, W., and Glassmeier, K.-H.: Mirror-mode-like structures in Venus' induced magnetosphere, J. Geophys. Res., 113, https://doi.org/10.1029/2008JE003154, 2008.
Volwerk, M., Richter, I., Tsurutani, B., Götz, C., Altwegg, K., Broiles, T., Burch, J., Carr, C., Cupido, E., Delva, M., Dósa, M., Edberg, N. J. T., Eriksson, A., Henri, P., Koenders, C., Lebreton, J. P., Mandt, K. E., Nilsson, H., Opitz, A., Rubin, M., Schwingenschuh, K., Wieser, G. S., Szego, K., Vallat, C., Vallieres, X., Glassmeier, K. H.: Mass-loading, pile-up, and mirror-mode waves at comet 67P/Churyumov-Gerasimenko, Ann. Geophys., 34, 1–15, https://doi.org/10.5194/angeo-34-1-2016, 2016.
Wang, G. Q., Volwerk, M., Nakamura, R., Boakes, P., Zhang, T. L., Yoshikawa, A., and Baishev, D. G.: Flapping current sheet with superposed waves seen in space and on the ground, J. Geophys. Res.-Space, 119, https://doi.org/10.1002/2014JA020526, 2014.
Wang, G. Q., Zhang, T. L., Volwerk, M., Schmid, D., Baumjohann, W., Nakamura, R., and Pan, Z. H.: Mirror mode structures ahead of dipolarization front near the neutral sheet observed by Cluster, Geophys. Res. Lett., 43, https://doi.org/10.1002/2016GL070382, 2016.
Wang, G. Q., Volwerk, M., Zhang, T. L., Schmid, D., and Yoshikawa, A.: High-latitude Pi2 pulsations associated with kink-like neutral sheet oscillations, J. Geophys. Res.-Space, 122, https://doi.org/10.1002/2016JA023370, 2017.
Wu, M. Y., Lu, Q. M., Volwerk, M., Vörös, Z., Zhang, T. L., Shan, L. C., and Huang, C., A statistical study of electron acceleration behind the dipolarization fronts in the magnetotail, J. Geophys. Res. Space Physics, 118, 4804–4810, https://doi.org/10.1002/jgra.50456, 2013.
Xiao, S. D., Zhang, T. L., Wang, G. Q., Volwerk, M., Ge, Y. S., Schmid, D., Nakamura, R., Baumjohann, W., Plaschke, F.: Occurrence rate of dipolarization fronts in the plasma sheet: Cluster observations, Ann. Geophys., 35, https://doi.org/10.5194/angeo-35-1015-2017, 2017.
Yao, S. T., et al.: Observations of kinetic-size magnetic holes in the magnetosheath, J.

Geophys. Res.-Space, 122, 1990–2000, doi:10.1002/2016JA023858, 2017.

Zhang, T. L., Russell, C. T., Baumjohann, W., Jian, L. K., Balikhin, M. A., Cao, J. B., Wang, C., Blanco-Cano, X., Glassmeier, K. H., Zambelli, W., Volwerk, M., Delva, M., Vörös, Z.: Characteristic size and shape of the mirror mode structures in the solar wind at 0.72 AU, Geophys. Res. Lett., 35, https://doi.org/10.1029/2008GL033793, 2008.

Zhang, T. L., Baumjohann, W., Russell, C. T., Jian, L. K., Wang, C., Cao, J. B., Balikhin, M., Blanco-Cano, X., Delva, M., and Volwerk, M.: Mirror mode structures in the solar wind at 0.72 AU, J. Geophys. Res., 114, https://doi.org/10.1029/2009JA014103, 2009.

Zhang, L., He, J. S., Zhao, J. S., Yao, S., and Feng, X. S.: Nature of magnetic holes above ion scales: a mixture of stable slow magnetosonic and unstable mirror modes in a double - polytropic scenario?, Astrophys. J., 864, 35. https://doi.org/10.3847/1538‐4357/aad4aa, 2018.

Zieger, B., Retinò, A., Nakamura, R., Baumjohann, W., Vaivads, A., and Khotyaintsev, Y.: Jet front-driven mirror modes and shocklets in the near-Earth flow-braking region, Geophys. Res. Lett., 38, https://doi.org/10.1029/2011GL049746, 2011.

Author contribution

Guoqiang Wang and Tielong Zhang designed the main idea of this study, and and the data analysis was mainly performed by Guoqiang Wang. Guoqiang Wang prepared the manuscript with contributions from all co-authors.

Acknowledgements

This work in China was supported by NSFC grants 41804157, 41774171, 41974205, 41774167, and 41904156. The authors also acknowledge the financial supported by the grant from Key Laboratory of Lunar and Deep Space Exploration, CAS, Shenzhen Science and Technology Research Program (JCYJ20180306171918617), and the 111 project [B18017]. We acknowledge the data from the NASA MMS mission. We also acknowledge MMS project FGM and FPI teams. The data of the MMS spacecraft are publicly available at https://lasp.colorado.edu/mms/sdc/public/.

Code/Data availability

The data of the MMS spacecraft are publicly available at https://lasp.colorado.edu/mms/sdc/public/.

Competing interests

The authors declare that they have no conflict of interest.